







Seepage field distribution and water inflow laws of tunnels in water-rich regions

LI Zheng^{1,3,4}  <https://orcid.org/0000-0002-6450-6604>; e-mail: tunnel1987@163.com

CHEN Zi-quan^{2*}  <https://orcid.org/0000-0002-8652-7561>;  e-mail: chenziqian@swjtu.edu.cn

HE Chuan²  <https://orcid.org/0000-0003-3551-5314>; e-mail: chuanhe12@163.com

MA Chun-chi^{2,5}  <https://orcid.org/0000-0002-5852-8022>; e-mail: machunchi17@cdut.edu.cn

DUAN Chao-ran⁶  <https://orcid.org/0000-0003-0337-1088>; e-mail: duancr@czust.com

*Corresponding author

1 School of Civil Engineering, Chongqing University, Chongqing 400045, China

2 Key Laboratory of Transportation Tunnel Engineering, Ministry of Education, Southwest Jiaotong University, Chengdu 610031, China

3 Chongqing University Industrial Technology Research Institute, Chongqing 401329, China

4 Chongqing City Construction Investment (Group) Co., Ltd, Chongqing 400023, China

5 State Key Laboratory of Geohazard Prevention and Geoenvironment Protection, Chengdu University of Technology, Chengdu 610059, China

6 School of Civil Engineering, Changzhou Institute of Technology, Changzhou 213032, China

Citation: Li Z, Chen ZQ, He C, et al. (2022) Seepage field distribution and water inflow laws of tunnels in water-rich regions. *Journal of Mountain Science* 19(2). <https://doi.org/10.1007/s11629-020-6634-x>

© Science Press, Institute of Mountain Hazards and Environment, CAS and Springer-Verlag GmbH Germany, part of Springer Nature 2022

Abstract: Currently, the water inrush hazards during tunnel construction, the water leakage during tunnel operation, and the accompanying disturbances to the ecological environment have become the main problems that affect the structural safety of tunnels in water-rich regions. In this paper, a tunnel seepage model testing system was used to conduct experiments of the grouting circle and primary support with different permeability coefficients. The influences of the supporting structures on the water inflow laws and the distribution of the water pressure in the tunnel were analyzed. With the decrease in the permeability coefficient of the grouting circle or the primary support, the inflow rate of water into the tunnel showed a non-linear decreasing trend. In

comparison, the water inflow reduction effect of grouting circle was much better than that of primary support. With the increase of the permeability coefficient of the grouting ring, the water pressure behind the primary lining increases gradually, while the water pressure behind the grouting ring decreases. Thus, the grouting of surrounding rock during the construction of water-rich tunnel can effectively weaken the hydraulic connection, reduce the influence range of seepage, and significantly reduce the decline of groundwater. Meanwhile, the seepage tests at different hydrostatic heads and hydrodynamic heads during tunnel operation period were also conducted. As the hydrostatic head decreased, the water pressure at each characteristic point decreased approximately linearly, and the water inflow rate also had a gradual downward trend. Under the action of hydrodynamic head, the water pressure had an

Received: 15-Dec-2020

Revised: 01-Jun-2021

Accepted: 10-Sep-2021

obvious lagging effect, which was not conducive to the stability of the supporting structures, and it could be mitigated by actively regulating the drainage rate. Compared with the hydrostatic head, the hydrodynamic head could change the real-time rate of water inflow to the tunnel and broke the dynamic balance between the water pressure and water inflow rate, thereby affecting the stress state on the supporting structures.

Keywords: Water-rich tunnel; Seepage field distribution; Water inflow law; Construction period; Operation period

1 Introduction

With the continuous development of infrastructure construction of China, the ground transportation system has been unable to satisfy the increasing demand of traffic volume, resulting in ground traffic congestion and low operational efficiency. As an effective utilization form of underground space, transportation tunnel engineering plays a very significant role in improving land-use efficiency, alleviating ground traffic, reducing environmental pollution, maintaining urban historical and cultural landscape. Thus, it has become the focus of modern construction to deal with traffic (Valdenebro and Gimena 2018; Yang and Peng 2016). Although it has many of the same characteristics as railway tunnels and highway tunnels, urban tunnels also possess many unique features when their functional diversity and special geographical positions are considered. First, due to the limitations of topography and existing buildings, the depths at which urban tunnels are buried usually are shallow, and the strength of the surrounding rock and its permeability resistance often are poor (Shi et al. 2017). Even so, urban tunnels often are built with large cross-sections in order to solve the problem of urban traffic congestion. Thus, forming a flat, large-section structure presents increased difficulty in both design and construction (Song et al. 2019). In addition, the hydrogeological conditions in urban areas often are complex, and hazards occur frequently in the processes of constructing and operating such tunnels (Liang et al. 2016; Li et al. 2019). In urban areas, the groundwater level often is high, and the abundant sources and complex seepage paths make the deformation mechanisms of the surrounding rock

and the evolution of the seepage field more unpredictable during the excavation for the tunnel (Fang et al. 2016; Gattinoni and Scesi 2017; Li et al. 2009). Therefore, as shown in Fig. 1, water intruding hazards, water leakage accidents and associated collapse of the surrounding rock were frequently encountered during tunnel excavation in water-rich regions (Perazzelli et al. 2014; Shen et al. 2013; Shi et al. 2018; Tan et al. 2018; Liu 2014; Li et al. 2013).

The statistics of 57 tunnels with safety problems during the construction period in China, indicate that water hazards are the most common problem since they occur in 58% of the tunnels (Zou et al. 2013). Irrespective of whether the tunnels are long-term or short-term tunnels, water inflow may lead to the decrease of the groundwater level, the depletion of the sources of surface water, followed by the erosion of the soil and the collapse of the ground. For tunnel structures, water leakage could accelerate the corrosion of bolts and the steel arch (Ma et al. 2019). It also can erode the auxiliary facilities in the tunnel and worsen the driving environment. Therefore, solving the problem of water inflow in urban tunnels would ensure the safety of tunnel construction and protect the surrounding ecological environment.

For specific projects, waterproof systems and water drainage in tunnels have become key factors for tunnel support structures. But considering the complex hydrogeological conditions of urban tunnels in water-rich regions, the processes by which underground seepage fields evolve in each stage of tunnel construction are different, which makes it difficult to effectively determine the actual state of the surrounding rock-supporting system. In addition, the problem of water inflow to the tunnel also involves the symbiosis and coordination of the groundwater and the surrounding environment, which should be studied in combination with waterproof systems (Hassani et al. 2016 and 2018). Hence, the evolution of water inflow, the influence of the support structure on intruding water, and the water pressure distribution in both the construction and operation periods of urban tunnels are all problems that have to be solved (Jiang et al. 2017; Liu et al. 2015; Wang et al. 2008; Zhang et al. 2018).

Many scholars have carried out research on related issues. Harr (1962) used the image method to analyze the distribution of pore water pressure in the rock surrounding an unlined tunnel. Li et al. (2009) analyzed the seepage field of a double-arch tunnel and



Fig. 1 Tunnel water hazards in China: (a), (b), (c) in construction period; (d), (e), (f) in operation period; (g), (h), (i) ground hazards caused by tunnel construction.

a twin-tube tunnel, proposing an innovative water-gathering system for tunnel water drainage. Fernandez and Moon (2010) studied the excavation-induced hydraulic conductivity reduction around a tunnel employing theoretical analysis and provided a guideline for estimating the ground water inflow rate. Liu et al. (2015) studied the seepage field of underwater tunnels, obtaining the spatial distribution of pore water pressure of the tunnel grouting circle and the lining in different drainage conditions. The above results provide the background for the study of the seepage field distribution and water inflow laws of tunnels in water-rich regions, but there remain several problems or defects. The existing theories are mainly based on the analysis of the seepage evolution in unlined tunnels, without regard for the surrounding rock, the grouting circle or the lining. The scope of studies are concentrated on the outside of the lining or the range of the grouting circle. There are limited studies on the spatial distribution of pore

water pressure in the surrounding rock and the affected areas of the seepage field. Meanwhile, it is also less studied by means of fine model test. Therefore, it is necessary to develop a seepage test device including surrounding rock support system to reveal the influence of grouting circle and supporting structures on seepage field distribution and water inflow laws of tunnels in water-rich regions.

In this paper, the connecting line of the Shenzhen eastern border crossing expressway, which is a typical urban tunnel in a water-rich region and has undergone serious water inflow problems during both the construction and operation periods, is used as a case study to investigate the water inflow laws. Using the tunnel seepage model testing system, we conducted seepage field tests in both the construction period and the operation period. The effect of the permeability coefficient of the grouting circle and the primary support on the inflow of water were investigated, and the distribution of the water

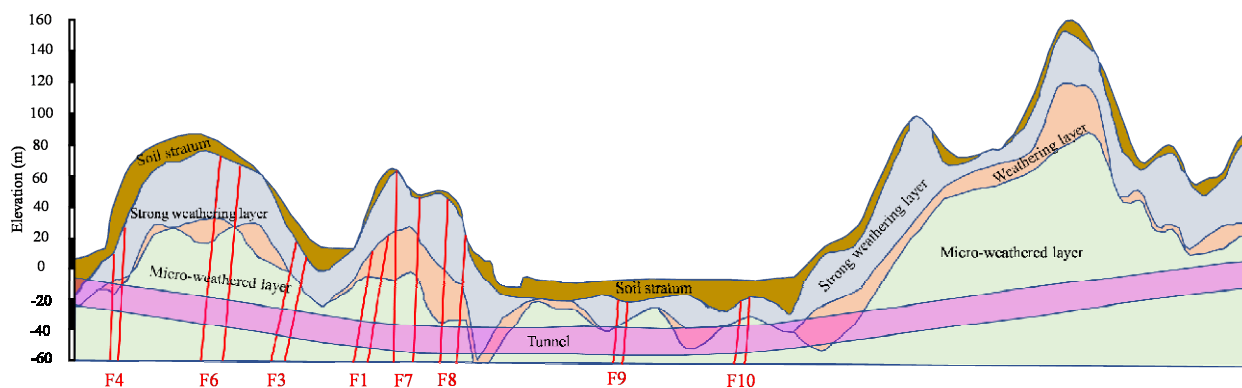


Fig. 2 Longitudinal profile of the connecting line of the Shenzhen eastern border crossing expressway. Note: F1, F3, F4, F6, F7, F8, F9, F10 were the faults distributed in the project area.

pressure for different grouting circles were analyzed. For comparison, we also studied the evolution of the seepage field and the water inflow laws during the operation of the tunnel under different hydrostatic and hydrodynamic heads.

2 Engineering Background and Experimental Methods

2.1 Engineering background

The connecting line of the Shenzhen eastern border crossing expressway is located in the Luohu District of Shenzhen City, China. This project is a large-scale underground interchange, composed of two parallel main tunnels (the South and North lines) and ramps, with a total length of about 8.6 km. Since the tunnel is adjacent to the Shenzhen reservoir (the north line is only 260 m away from the reservoir dam) and the entire tunnel is below the groundwater level, the hydrogeological conditions along the tunnel are very complicated. After excavation, the Shenzhen reservoir in the North could recharge the groundwater of the tunnel and form new seepage paths, which could induce water inrush hazards. In addition, the microtopography along the tunnel is developed, mainly including rolling hills and diluvial upland, and the lithology consists of an artificial accumulation of a layer of soil consisting of quaternary holocene and medium to slightly-weathered carboniferous metamorphic rocks (Fig. 2). In addition, many faults with different scales pass through the tunnel, and the surrounding rock has developed fractures. Hence, rich groundwater resources, together with complicated geological structures and hydrogeological conditions,

resulted in water leakage and water inflow problems in the tunnel during the construction period. And due to the limited discharge method that was used, the volume of the drainage during the operation of the tunnel was amazing.

In order to investigate the water inflow laws and their influence on urban tunnels in water-rich regions, section NXK2 + 980 in the connecting line of the Shenzhen eastern border crossing expressway was selected as the test site because it was the closest to the Shenzhen reservoir. The width and height of the tunnel section were 14.2 and 9.8 m, respectively. Its buried depth was about 40.4 m, and the water level was just 10.6 m below the surface of the ground. The fissures and joints were well developed in the surrounding rock and in the section located in the small-scale secondary fracture concentrated zone. Based on the results of drainage and injection field tests, the average permeability coefficient of the surrounding rock was as high as 0.135 m/d (Li et al. 2019). All of these factors, in combination with the poor physical and mechanical properties of the surrounding rock, led to a large amount of inrushing water after the excavation of the tunnel, and the supporting structures had to withstand significantly high external water pressure (Fig. 3). Hence, it can be seen that the prediction of water inflow to the tunnel during its construction and operational period and the study of the influence of the grouting circle and other supporting effects on the water inflow were vitally important to ensure the safety of the tunnel.

2.2 Experimental device

An experimental study of the water inflow laws of urban tunnels in water-rich regions during their

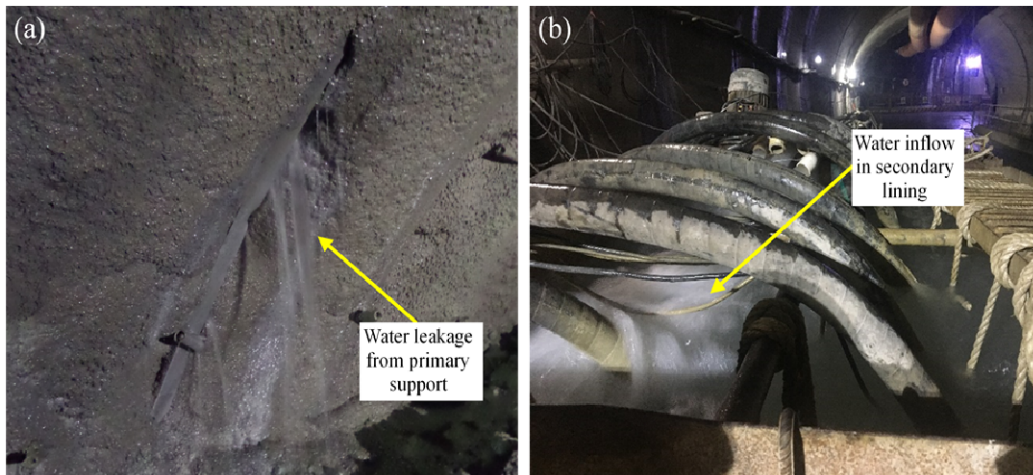


Fig. 3 Water inflow problems during the construction of the connecting line of the Shenzhen eastern border crossing expressway: (a) water leakage from primary support; (b) water inflow in secondary lining.

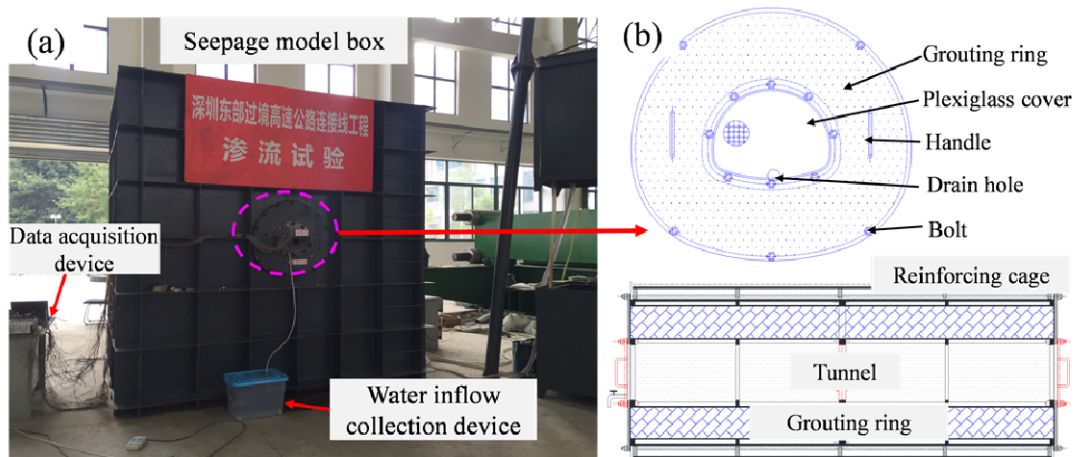


Fig. 4 Tunnel seepage model testing system: (a) overall model; (b) supporting structures.

construction and operation periods was conducted using the tunnel seepage model testing system (Fig. 4). This system consisted of a seepage model box, a simulation device for the reinforcement area, an anti-filter layer, a height-adjustable circulating water tank, a water inflow collecting device, and a data acquisition device. The seepage model box was composed of 10-mm-thick stiffened steel plates, and both the front and rear sides were equipped with horseshoe-shaped door openings. According to the geometric similarity ratio of 1:30, the tunnel was 430 mm wide and 330 mm high, which was about 4 times the hole diameter from the side wall to eliminate the influence of the seepage boundary. The door opening was equipped with a double-layer flange plate that had two rings of internal and external bolts. The lower side of the plexiglass cover plate was equipped with a switch for collecting water.

In the process of preparing for the test, similar materials of surrounding rock made of clay, fine sand, and glass fibers were layered in the seepage model box. The device used to simulate the reinforcement area was connected at the hole of the seepage model box through a double-layer flange, and the tunnel structures, such as the primary and secondary linings, were placed successively in the model box. The grouting circle was prefabricated using a special mold, and it was connected by blocks to fill the reinforcement area, which was covered externally by a filter layer composed of non-woven fabric and plastic mesh to form a stable working area. The movable, circulating water tank provided the water head for the test. While the water pressure test system and water inflow collection device could collect the test data effectively. Thus, the above devices form a complete seepage test system for urban tunnels in water-rich

regions.

2.3 Experimental similar materials

The core of the model test in this paper was to study the laws of water inflow during the construction period and the operation period based on the groundwater seepage theory. Theoretically, the water inflow is mainly controlled by the tunnel diameter, water pressure, seepage influence radius, permeability coefficient of surrounding rock and the supporting structures (Li et al. 2019), but it is not related to the physical and mechanical properties of the surrounding rock, the grouting circle, or the primary support. Therefore, taking control of the permeability coefficient of similar materials as the comprehensive index, according to the second similarity theorem, the dimensional analysis method was used to determine the test similarity ratio, as shown in Table 1. The similarity ratio is based on the permeability coefficient similarity ratio, the geometric similarity ratio, and gravity similarity ratio.

In this paper, the research core is the seepage field distribution and water inflow laws of tunnels. Whereas the water pressure and drainage value are mainly related to the parameters such as tunnel diameter, acting head, seepage influence radius, the permeability coefficient of surrounding rock and supporting system, it has little relationship with the mechanical properties of surrounding rock, grouting ring, primary lining and other materials. Therefore, the mechanical properties and deformation stability of surrounding rock and supporting system are ignored in this paper. Taking the control of the permeability coefficient of similar materials as the core, it is considered that the secondary lining is an impermeable structure, and the water infiltrating into the primary lining is derived and collected through the drainage system, so as to study the change law of

Table 1 The similarity ratios of the materials

Similarity ratio	Formula	Value
Geometric	$C_L = l_m / l_p$	30
Permeability coefficient	$C_K = k_m / k_p$	1
Specific weight	$C_\gamma = \gamma_m / \gamma_p$	1
Head height	$C_H = C_L$	30
Time	$C_t = \frac{C_H}{C_K}$	30
Water pressure	$C_p = C_\gamma C_H$	30
Drainage	$C_Q = \frac{C_H^3}{C_t}$	900

Notes: l_m , k_m and γ_m are the geometric, permeability coefficient and specific weight of the engineering prototype, while l_p , k_p and γ_p are the those in the model test.

the tunnel drainage and water pressure, etc.

In the test, clay with small permeability coefficient and fine sand with large permeability coefficient were proposed to be used for the similar materials of surrounding rock, and glass fiber with high elastic coefficient and tensile strength and low water absorption is appropriately added to enhance its cohesion. So as to avoid the formation of through cracks in the prepared surrounding rock when encountering water and make the permeability more uniform. The permeability coefficient of surrounding rock is measured by a variable head tester in Fig. 5. As for the grouting circle, which effectively reduces the permeability coefficient of surrounding rock and enhances its water seepage resistance capacity, the Portland cement and carbon slag (particle size $\leq 2\text{mm}$) were selected to be used in this test (Fig. 6). Besides, the woven geotextile with certain permeability was proposed to simulate the primary support of similar materials. Considering the actual primary support



Fig. 5 Preparation of similar materials for surrounding rock.



Fig. 6 Preparation of similar materials for grouting circle.

Table 2 Ratio of similar materials in model test

Tunnel structure	Surrounding rock	Grouting circle	Primary support	Secondary lining
Permeability coefficient (m/d)	0.135	0.016	8.64×10^{-3}	8.64×10^{-4}
Ratio of similar materials	Clay: fine sand: glass fiber=1: 1.4: 0.01	Cement: carbon slag=1: 10, thickness=150 mm	8-layer woven geotextiles, thickness=5.924 mm	1: 1.3 special plaster (steel mesh inside)+3 mm waterproof varnish

Table 3 Seepage tests under different grouting circle and primary support permeability coefficients

Supporting structure	Primary support	Grouting circle
Case 1	no	no
Case 2	Permeability coefficient 8.64×10^{-3} m/d (8-layer woven geotextile, thickness 5.924 mm)	Permeability coefficient 28×10^{-3} m/d (Cement: carbon slag=1: 12, thickness 150 mm)
Case 3	Permeability coefficient 8.64×10^{-3} m/d (8-layer woven geotextile, thickness 5.924 mm)	Permeability coefficient 16×10^{-3} m/d (Cement: carbon slag=1: 10, thickness 150 mm)
Case 4	Permeability coefficient 8.64×10^{-3} m/d (8-layer woven geotextile, thickness 5.924 mm)	Permeability coefficient 6×10^{-3} m/d (Cement: carbon slag=1: 6, thickness 150 mm)
Case 5	Permeability coefficient 12.5×10^{-3} m/d (6-layer woven geotextile, thickness 4.443 mm)	Permeability coefficient 16×10^{-3} m/d (Cement: carbon slag=1: 10, thickness 150 mm)
Case 6	Permeability coefficient 7.35×10^{-3} m/d (12-layer woven geotextile, thickness 8.886 mm)	Permeability coefficient 16×10^{-3} m/d (Cement: carbon slag=1: 10, thickness 150 mm)

permeability coefficient is about 8.64×10^{-3} m/d, while the permeability coefficient of single-layer geotextile is $0.303 \sim 0.371$ m/d, so the comprehensive permeability coefficient is tested in the form of multi-layer stacking to meet the demand. Combined with the material parameters tested in the project site, using the self-made special equipment, and through a large number of proportion tests, we determined the new similar materials, such as the surrounding rock, grouting circle, primary support, and their proportion of raw materials suitable for the seepage test of tunnel (Table 2).

2.4 Test procedure of the construction period

The reasonable prediction of the inflow of water to the tunnel is related to the selection of grouting measures, the determination of the pressure of the water behind the supporting structures, the type of waterproofing and drainage systems in the tunnel.

For urban tunnels constructed by the mining method in water-rich areas, the grouting circle and primary support are the most important components of the tunnel's waterproof system, which could directly affect the seepage field distribution and water pressure on the supporting structures (Arjnoi et al. 2009). Commonly, compared with the thickness effect, the permeability coefficients of the grouting circle and the primary support are the important factors that affect the seepage field distribution during the construction period. Therefore, in order to study the influence of the supporting structure on the water inflow laws of urban tunnels in water-rich regions, seepage tests were conducted for different grouting circles and different primary support permeability coefficients. Table 3 lists all of the test conditions, in which case 1 is unsupported, cases 2, 3, 4 could analyze the influence of different grouting circles, and cases 3, 5, 6 could analyze the primary support permeability coefficients.



Fig. 7 Photos of test procedure: (a) embedding of grouting circle; (b) install supporting structures; (c) backfill surrounding rock; (d) unexcavated surrounding rock; (e) non-disturbed excavation state; (f) water inflow collection; (g) moist state (seepage for 27 h in case 3); (h) water dripping state (seepage for 49 h in case 3); (i) linear gushing water state (seepage for 64 h in case 3).

During the construction period, the tunnel water inflow laws belong to the unsteady seepage distribution problem. With the excavation of the tunnel, the damage to the surrounding rock develops gradually, and the water diversion capacity is strengthened continuously. This process is very complex and difficult to simulate effectively. In order to simplify the study, in this paper, the excavation process was ignored when analyzing the water inflow laws during the construction period. Various measures, such as timely grouting around the and full-face curtain grouting in front of the face of the tunnel, were used to reduce the disturbance to the surrounding rock. Fig. 7 shows that, first of all, the temporary partition board of the face of the tunnel, the grouting circle, and the primary support were installed successively in the double-layer reinforcement cage at the middle of the model box. Then, the filter layer was laid outside the

reinforcement cage and in front of the tunnel face, and the full-face curtain grouting area was set close to the inverted filter layer. Next, the surrounding rock in the model box and in front of the tunnel was backfilled to form the construction state without considering the influence of any disturbance caused by the excavation. Then, the double-layer flange plate and model box top cover were closed, and waterproof sealing rubber was applied to each component and the bolt interface to ensure water tightness. Finally, a stable head of test water was ensured to supply to the model by controlling the movable circulating water tank device, and the inflow of water to the tunnel was measured.

Fig. 8 shows the sketch map of the non-disturbed excavation, and the experiment studied the water inflow during the construction period of the urban tunnel without considering the influence of excavation disturbance; since the test is a local

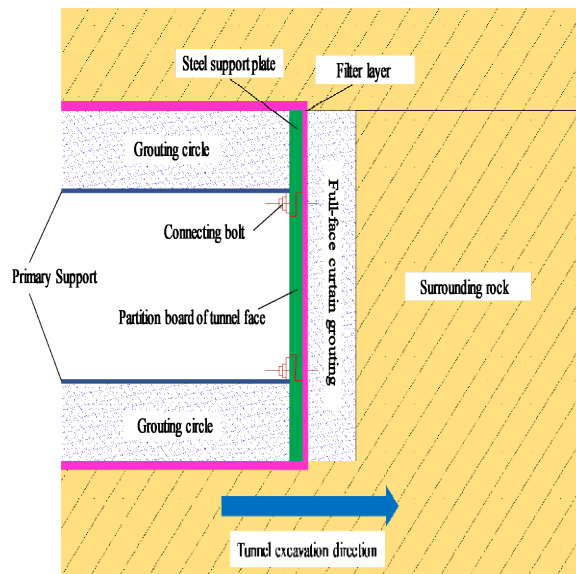


Fig. 8 Sketch map of non-disturbed excavation.

Table 4 Seepage tests under different water heads

Water pressure type	Initial heads (m)	Surrounding rock	Grouting circle	Primary support	Secondary lining
Hydrostatic head	20, 25, and 30	0.135	0.016	8.64×10^{-3}	8.64×10^{-4}
Hydrodynamic head	20, 25, and 30	0.135	0.016	8.64×10^{-3}	8.64×10^{-4}

seepage model, the water head can be considered as an infinite recharge effect. The water inflow was collected by connecting the water transfer hose with the water regulating valve and the water tank with a scale.

2.5 Test procedure of the operation period

When the environment of the tunnel site is stable, the tunnel is under the action of static water head for a long time during the operation period, and the supply, seepage, and discharge of groundwater reach a dynamic balance. The stress of the tunnel structure is clear, and the relationship between water pressure and drainage is constant. However, when the tunnel groundwater environment changes, such as the discharge of flood water from the reservoir and local heavy rainfall, the tunnel will be affected by the dynamic head. At this time, the original balance of the seepage field is broken, and the relationship between the water pressure and the drainage volume of the tunnel changes (Li et al. 2018). Especially for urban tunnels with shallow buried depth in water-rich regions, the sudden change of the water head may disturb the equilibrium state between the

surrounding rock and the supporting system.

With the whole lifecycle of the tunnel, the effect of the head of groundwater on the seepage field of the tunnel is the most direct effect. In order to effectively solve the problem of long-term tunnel seepage, it is necessary to study the influence of the water head on the relationship between the water pressure and the water inflow of the tunnel in order to analyze the evolution process of the underground seepage field of the tunnel (Farhadian and Nikvar-Hassani 2019). The tunnel seepage model test method can reflect the actual situation of the project directly. It is an important means of studying the evolution of the underground seepage field, the influence of water pressure on the structure of the tunnel, and predicting the water inflow characteristics of the tunnel. Hence, using the tunnel seepage model testing system (Fig. 5), experiments are conducted for different hydrostatic heads and hydrodynamic heads during the period when the tunnel is in operation. The simulations of hydrostatic head and hydrodynamic head are achieved by adjusting the movable, circulating water tank. Table 4 shows that, in this test, the initial heads were set at 20, 25, and 30 m, respectively. Among the initial heads, when water is

introduced into the mobile water tank from the fixed water tank to form a circulation and maintain stability, the static head effect of the tunnel is simulated. However, after the water pressure and drainage value of the tunnel displayed by the data acquisition device are stable, the submersible pump is stopped thereby stopping the supply of groundwater, and this makes the acting head decreases naturally with time depending on the discharge capacity of the tunnel itself, thereby simulating the hydrodynamic head. Its initial water head is the same as the test value of the static head.

3 Water Inflow Laws During the Construction Period

3.1 Effect of supporting structures

The stratum lithology of the selected section NXX2+980 in the connecting line of the Shenzhen eastern border crossing expressway mainly was medium-weathered, carboniferous metamorphic rocks. The tunnel passed through small-scale secondary fracture in dense zone F5, where the fracture developed in the surrounding rock. In addition, groundwater activities were frequent, especially in the fracture intensive zone, which easily can become a potential channel for groundwater to penetrate into the tunnel. Therefore, as the important parts of the waterproofing system for the tunnel, the grouting circle and primary support, which could determine the distribution of the seepage field and the water pressure on second lining after the excavation of the tunnel, became the core to ensure the safety of the tunnel.

Fig. 9 shows the test results under six conditions when the tunnel is in an unsupported state without considering the influence of excavation disturbance (case 1), the water inflow rate is the largest, and the average water inflow rate is up to 11.38 m³/(d·m). The

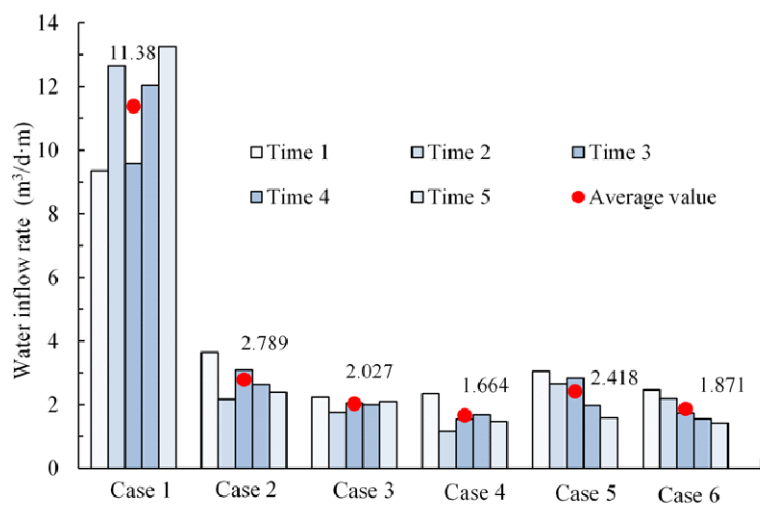


Fig. 9 Test results under different grouting circle and primary support permeability coefficients.

water inflow rate could be reduced significantly after the grouting circle and the primary support have been installed. With the decrease of the permeability coefficient of the grouting circle or the primary support, the average water inflow rate underwent a non-linear decrease. In contrast, the influence on the water inflow rate of reducing the permeability coefficient of the grouting circle was more obvious. The average values of the test for cases 2, 3, and 4 were 2.789, 2.027 and 1.664 m³/(d·m). From case 2 to case 3 and from case 3 to case 4, the average water inflow rate was reduced by 27.3% and 17.9%, respectively, whereas the average values of the tests for cases 5, 3, and 6 were 2.418, 2.027 and 1.871 m³/(d·m). From the 6-layer to the 8-layer and from the 8-layer to the 12-layer woven geotextile, the average water inflow rate was reduced by 16.2% and 7.7%, respectively. It can be seen that the grouting circle had a prominent water resistance effect, and reducing its permeability coefficient was the controlling role in improving the water inflow during the construction of the tunnel.

During the test, the face of the tunnel was the main source of water inflow, while the grouting circle or primary support was mainly dripping water with an occasional, linear gushing water state. With the decrease of the permeability coefficient, the discreteness of single water inflow rate measured under different conditions also decreased. However, when the permeability coefficients of the grouting circle and the primary support were changed, the change rule of water inflow rate of continuous collection was not the same. By changing the

permeability coefficient of the grouting circle, first, the water inflow results of continuous collection under various conditions decrease, and then they increase to gradually balance. This shows that the saturation of the grouting circle takes a long time, and the internal water pressure increases to a certain extent, making the channels that originally were closed gradually become dredged, which has a great impact on the groundwater seepage field around the tunnel. When the permeability coefficient of the primary support is changed, the results of continuous collection of water inflow under various conditions gradually decrease until balance is attained.

3.2 Water pressure distribution

To protect the environment and reduce the water pressure on supporting structures, the controlled drainage principle is used mainly in urban tunnels and mountain tunnels that have high levels of water. The purpose is to control the dynamic balance relationship between the external water pressure on the secondary lining and the drainage volume of the tunnel. Grouting reinforcement, as a conventional auxiliary means in tunnel construction, can seal the fractured rock mass effectively within the scope of reinforcement, thus reducing the permeability of the surrounding rock, blocking the supply of pore water to the tunnel, and enhancing the stability of the surrounding rock. Existing studies have shown that increasing the thickness of the grouting circle reduces the water pressure in the lining, while the influence of the permeability of the grouting circle on the water pressure and seepage state in the tunnel has not been determined to date (Fernandez and Moon 2010).

Therefore, in order to determine the effect of the

permeability coefficient of the grouting circle on the distribution of water pressure, the water pressures of the inner and outer sides of the grouting circle are tested under cases 2, 3, and 4. Fig. 10(a) shows that the water pressure of the vault near the tunnel excavation area is decreasing rapidly, but it is not zero, which indicates that there is still dynamic water pressure near the face of the tunnel during the construction period. The speed at which the water pressure decreases at inner part of the grouting circle is much faster than that the speed at the outer part. And the spatial effect of the change in the water pressure near the face of the tunnel is more significant; the minimum value of water pressure at the inner side of the grouting circle, which is about 2 m from the face of the tunnel, was only 32.55 kPa. Within the excavated area of the tunnel, the water pressure behind the primary support increases as the permeability coefficient of the grouting circle increases, and the water pressure behind the grouting circle decreases. The closer to the tunnel face that the measurements are made, the lower the water pressure becomes. It can be seen that the excavation of the tunnel leads to a significant change in the original seepage field. In the surrounding rock of the unexcavated area, the water pressure of each measuring point increases as the distance from the face of the tunnel increases, and the change in the permeability coefficient of the grouting circle has limited influence on the distribution of the seepage field of the surrounding rock in front of the face of the tunnel.

Fig. 10(b) presents the water pressure distribution at the arch bottom of the tunnel, and the water pressure behind the primary lining increases gradually as the permeability coefficient of the

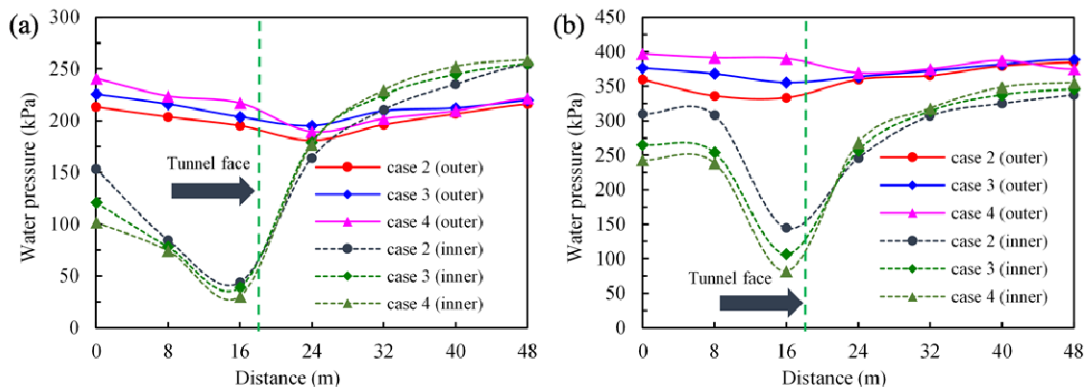


Fig. 10 Water pressure distribution of the inner and outer sides of the grouting circle during construction period: (a) vault; (b) arch bottom.

grouting circle increases, and the water pressure behind the grouting circle decreases. It can be seen that the pre-grouting measures during the construction period can reduce the water pressure on the secondary lining effectively. In the surrounding rock of the unexcavated area, the value of the water pressure at each measuring point behind the grouting circle changes very little with the permeability of the grouting circle.

4 Water Inflow Laws during Operation Period

4.1 Effect of hydrostatic head

The groundwater head has an important role in the evolution of the seepage field of the tunnel. In this test, the initial water heads were 20, 25, and 30 m, respectively. When the hydrostatic head was 30 m, the seepage evolution process of the inner wall of the grouting circle was obvious. About 20 h later, a small amount of block-wetted surface appeared, which was located mainly at the top and bottom of the arch, indicating that the underground water has begun to drain into the tunnel through the grouting circle. After 36 h of seepage, a few drops of water appeared at the arch crown. After 64 h of seepage, the frequency of the water drops increased, and the flow of water quickly became a gushing stream of water. After the hydrostatic head was reduced to 25 m and then to 20 m, a significant amount of time passed before the inner wall of the grouting circle was subjected to massive wetting and the saturation line was greatly extended. When the water head was 25 m, block wetting occurred after 31 h, and the water drops

on the arch crown drop after 60 h. When the water head was 20 m, a small amount of water drops could be seen on the arch crown after about 80 h. It was observed that, when the level of the groundwater decreased, the speed of the seepage became slower and the seepage time increased significantly.

Fig. 11(a) shows the distribution of the water pressure inside and outside the grouting circle of the tunnel under different hydrostatic heads. These measurements were made after the water pressure and the inflow of water were stable. Obviously, the water pressure distribution of each position changes for different values of the hydrostatic head. The variation law of water pressure inside and outside the grouting circle basically is the same, which shows the trend of gradually increasing from the vault to the bottom of the arch. For the same head of water, the water pressure behind the grouting circle at the same position of the tunnel is greater than that behind the secondary lining, which shows that the grouting circle has certain resistance to the water. When the hydrostatic head decreases, the pressure of the water at each point decreases approximately linearly, which indicates that the response of the tunnel to the change in the head of water is sensitive and consistent.

The value of the water inflow rate gradually trends downward (Fig. 11(b)) as the height of the water decreases. The heads of 30, 25, and 20 m correspond to water inflow rates to the tunnel of 0.478, 0.375, and 0.296 m³/(d·m), respectively. Through many tests, it was found that the lower the water head becomes, the smaller the dispersion of the test results becomes, indicating that the rate of water inflow to the tunnel is more stable under the effect of a low head of water.

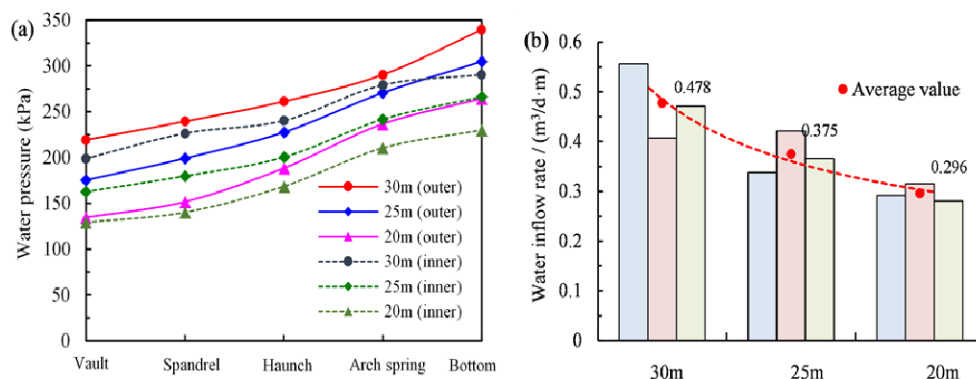


Fig. 11 Effect of hydrostatic head during tunnel operation period: (a) water pressure inside and outside the grouting circle; (b) average water inflow rate of three tests.

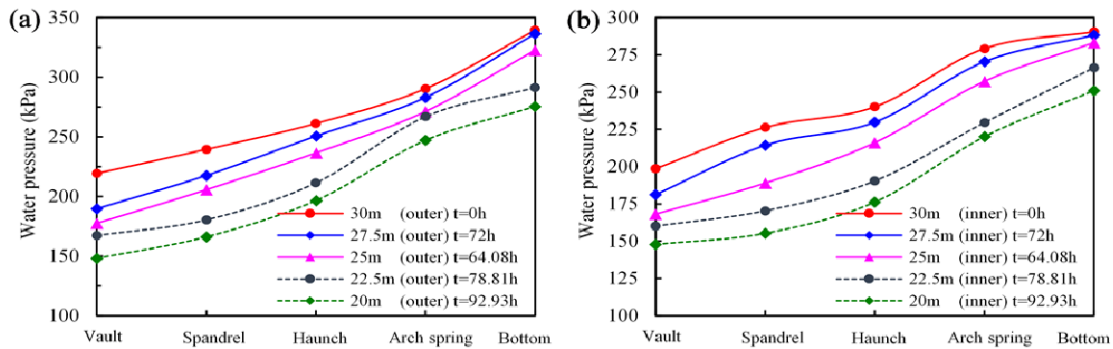


Fig. 12 Evolution of water pressure under 30 m hydrodynamic head: (a) outer of the grouting circle; (b) inner of the grouting circle.

4.2 Effect of hydrodynamic head

In the experiment to assess the process of tunnel seepage due to hydrodynamic head, we applied hydrostatic heads of 20, 25, and 30 m, respectively. When the water pressure and water inflow of the tunnel were stable, the supply of water head was stopped, and the hydrodynamic head simulation effect was achieved by relying on the natural process of decreasing the groundwater level over time.

As an example for analysis, Fig. 12 shows the evolution of the water pressure starting with an initial water head of 30 m. Compared with the results of hydrostatic head test, the water pressure was higher during the hydrodynamic head simulation effect. When the water head decreases to 20 m, the average water pressures at the outside and inside of the grouting circle were 206.7 and 190.1 kPa, respectively, which were 5.3% and 7.9% higher than that of the hydrostatic head. These results show that, under the action of dynamic head, the water pressure has an obvious lagging effect, which is not conducive to the stability of the supporting structures. And according to the saturated-unsaturated seepage control equation, when the water level is rising, the response of the groundwater also is delayed, and the dynamic water pressure increases. In the process of the level of the groundwater decreasing, the water pressure at the vault position changes the fastest, while the range of the change of the arch bottom position was smaller, which indicated that the shallow buried part is more susceptible to the impact of the dynamic water head.

Fig. 13 shows that the water inflow rate decreases with time. When the hydrodynamic head was 30 m, the water inflow rate of the tunnel reached 0.478 m³/(d·m). As the water head decreased to 20 m, the

rate decreased to 0.339 m³/(d·m), but it is still larger than the value of 0.296 m³/(d·m) that was observed under hydrostatic head. Hence, compared with hydrostatic head, the hydrodynamic head will change the real-time water inflow rate of the tunnel and destroy the dynamic balance between the water pressure and water inflow rate, thereby influencing the water pressure on the supporting structures. In addition, the stability of the structure can be affected, so it is necessary to take active measures to control the water inflow rate to mitigate the impact.

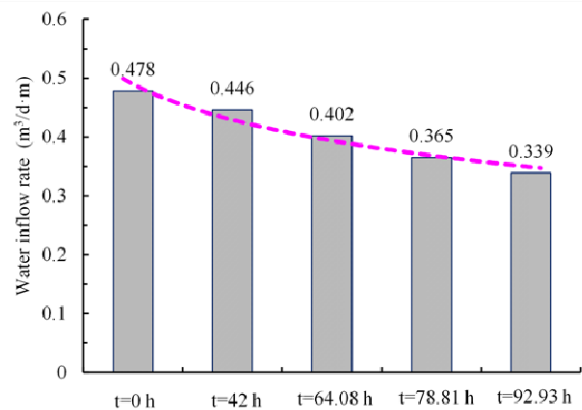


Fig. 13 Evolution of water inflow rate under 30 m hydrodynamic head.

With the increasing emphasis on environmental protection in China's engineering construction, it is of great significance to organically combine the efficient construction and safe operation of tunnel with the protection of groundwater environment. In general, through the development of the tunnel seepage model testing system, the seepage field tests in both the construction period and the operation period were conducted in this paper. It was found that a perfect waterproof system plays a significant role in

maintaining groundwater stability, can effectively weaken local hydraulic connection, reduce the influence range of seepage and avoid the rapid reduction of groundwater level. However, due to the limitation of test technology, only the influence of seepage field is considered in this paper. In the follow-up research process, the interaction between surrounding rock pressure and seepage field needs to be considered at the same time. Meanwhile, a large number of urban tunnels are often double tunnels, accompanied by the upper or lower crossing of existing tunnels. The interaction of seepage field between those tunnels also needs to be investigated. Moreover, to maintain the balance between the ecological environment of groundwater and the safety performance of tunnel structures, an active waterproof and drainage structure system will have important research significance in the future.

5 Conclusions

In this paper, we used the tunnel seepage model testing system to conduct seepage field tests in both the period when the tunnel was being constructed and when it was operational, and we studied the influence of the different permeability coefficients of the supporting structures and of different water heads on the water inflow laws of an urban tunnel in a water-rich region. The major conclusions of this study are as follows:

(1) With the decrease of the permeability coefficient of the grouting circle or the primary support, the water inflow rate to the tunnel had a non-linear, decreasing trend. In contrast, the influence of reducing the permeability coefficient of the grouting circle on the water inflow rate was about twice that of primary support. Thus, the grouting of surrounding rock during the construction of water-rich tunnel can effectively weaken the hydraulic connection, reduce the influence range of seepage, and significantly control the decline of groundwater.

(2) The pre-grouting measures during the construction period effectively can reduce the water

pressure on the secondary lining. With the increase of the permeability coefficient of the grouting circle, the water pressure behind the primary lining increased gradually, while the water pressure behind the grouting circle decreased. In the rock surrounding the unexcavated area, the water pressure behind the grouting circle hardly changed at all with the permeability of the grouting circle.

(3) With the decrease of the hydrostatic head, the water pressure of each characteristic point decreased approximately linearly, and the water inflow rate also had a gradual decrease. When the hydrostatic head became lower, the water pressures in the same positions of the secondary lining and the grouting circle were getting closer, and the dispersion of the inflow rate of water to the tunnel also was smaller, which indicated that the evolution of the seepage was more stable when the head of water was low.

(4) Under the action of the hydrodynamic head, the water pressure had an obvious lagging effect, and it will destroy the dynamic balance between tunnel water pressure and drainage, which was not conducive to the stability of the supporting structures. Also, the shallow buried place was more vulnerable to being affected by the process of the decreasing dynamic head and it can be mitigated by actively regulating the drainage rate during actual tunnel operation.

Acknowledgments

This research was supported by the Chongqing Natural Science Foundation (No. cstc2020jcyj-msxmX0904), the Chongqing Talent Plan (No. CQYC2020058263), the Chongqing Technology Innovation and Application Development Project (No. cstc2021ycjh-bgzxm0246), the China Postdoctoral Science Foundation (No. 2021M693739), the Sichuan Science and Technology Program (No. 2021YJ0539) and the Natural Science foundation of Jiangsu higher education institutions of China (Grant No.19KJD170001).

References

Arjanoi P, Jeong JH, Kim CY, Park KH (2009) Effect of drainage conditions on porewater pressure distributions and lining stresses in drained tunnels. *Tunn Undergr Sp Technol* 24:

376-389.

<https://doi.org/10.1016/j.tust.2008.10.006>

Fang Y, Guo JN, Grasmick J, Mooney M (2016) The effect of

- external water pressure on the liner behavior of large cross-section tunnels. *Tunn Undergr Space Technol* 60: 80-95.
<https://doi.org/10.1016/j.tust.2016.07.009>
- Farhadian H, Nikvar-Hassani A (2019) Water flow into tunnels in discontinuous rock: a short critical review of the analytical solution of the art. *Bull Eng Geol Environ* 78: 3833-3849.
<https://doi.org/10.1007/s10064-018-1348-9>
- Fernandez G, Moon J (2010) Excavation-induced hydraulic conductivity reduction around a tunnel-Part 1: Guideline for estimate of ground water inflow rate. *Tunn Undergr Space Technol* 25: 560-566.
<https://doi.org/10.1016/j.tust.2010.03.006>
- Gattinoni P, Seesi L (2017) The groundwater rise in the urban area of Milan (Italy) and its interactions with underground structures and infrastructures. *Tunn Undergr Space Technol* 62: 103-114.
<https://doi.org/10.1016/j.tust.2016.12.001>
- Harr ME (1962) *Groundwater and Seepage*. McGraw-Hill.
- Hassani AN, Katibeh H, Farhadian H (2016) Numerical analysis of steady-state groundwater inflow into Tabriz line 2 metro tunnel, northwestern Iran, with special consideration of model dimensions. *Bull Eng Geol Environ* 75: 1617-1627.
<https://doi.org/10.1007/s10064-015-0802-1>
- Hassani AN, Farhadian H, Katibeh H (2018) A comparative study on evaluation of steady-state groundwater inflow into a circular shallow tunnel. *Tunn Undergr Space Technol* 73: 15-25. <https://doi.org/10.1016/j.tust.2017.11.019>
- Jiang HM, Li L, Rong XL, et al. (2017) Model test to investigate waterproof-resistant slab minimum safety thickness for water inrush geohazards. *Tunn Undergr Space Technol* 62: 35-42.
<https://doi.org/10.1016/j.tust.2016.11.004>
- Liang DX, Jiang ZQ, Zhu SY, et al. (2016) Experimental research on water inrush in tunnel construction. *Nat Hazards* 81: 467-480.
<https://doi.org/10.1007/s11069-015-2090-2>
- Liu JG (2014) Research on tunnel drainage control based on ecological environment protection. *Mod Tunn Technol* 51: 61-66. (In Chinese)
<https://doi.org/10.13807/j.cnki.mtt.2014.03.010>
- Liu Q, Tan ZS, Wang XY (2015) Model test study on the distribution law of underwater tunnel seepage field. *China Civ Eng J* 48: 388-392. (in Chinese)
[https://doi.org/10.1000-131X\(2015\)S1-0388-05](https://doi.org/10.1000-131X(2015)S1-0388-05)
- Li D, Li X, Li CC, et al. (2009) Case studies of groundwater flow into tunnels and an innovative water-gathering system for water drainage. *Tunn Undergr Space Technol* 24: 260-268.
<https://doi.org/10.1016/j.tust.2008.08.006>
- Li T, Mei TT, Sun XH, et al. (2013) A study on a water-inrush incident at Laohutai coalmine. *Int J Rock Mech Min Sci* 59: 151-159.
<https://doi.org/10.1016/j.ijrmms.2012.12.002>
- Li PF, Wang F, Long YY, Zhao X (2018) Investigation of steady water inflow into a subsea grouted tunnel. *Tunn Undergr Space Technol* 80: 92-102.
<https://doi.org/10.1016/j.tust.2018.06.003>
- Li Z, He C, Chen ZQ, et al. (2019) Study of seepage field distribution and its influence on urban tunnels in water-rich regions. *Bull Eng Geol Environ* 76: 4035-4045.
<https://doi.org/10.1007/s10064-018-1417-0>
- Ma D, Duan HY, Li XB, et al. (2019) Effects of seepage-induced erosion on nonlinear hydraulic properties of broken red sandstones. *Tunn Undergr Space Technol* 91: 102993.
<https://doi.org/10.1016/j.tust.2019.102993>
- Perazzelli P, Leone T, Anagnostou G et al. (2014) Tunnel face stability under seepage flow conditions. *Tunn Undergr Space Technol* 43: 459-469.
<https://doi.org/10.1016/j.tust.2014.03.001>
- Shen SL, Ma L, Xu YS, et al. (2013) Interpretation of increased deformation rate in aquifer IV due to groundwater pumping in Shanghai. *Can Geotech J* 50: 1129-1142.
<https://doi.org/10.1139/cgj-2013-0042>
- Shi CH, Cao CY, Lei MF (2017) Construction technology for a shallow-buried underwater interchange tunnel with a large span. *Tunn Undergr Space Technol* 70: 317-329.
<https://doi.org/10.1016/j.tust.2017.09.009>
- Shi SS, Xie XK, Bu L, et al. (2018) Hazard-based evaluation model of water inrush disaster sources in karst tunnels and its engineering application. *Environ Earth Sci* 77: 141.
<https://doi.org/10.1007/s12665-018-7318-5>
- Song SG, Li SC, Li LP, et al. (2019) Model test study on vibration blasting of large cross-section tunnel with small clearance in horizontal stratified surrounding rock. *Tunn Undergr Space Tech* 92: 103013.
<https://doi.org/10.1016/j.tust.2019.103013>
- Tan YQ, Smith JV, Li CQ, et al. (2018) Predicting external water pressure and cracking of a tunnel lining by measuring water inflow rate. *Tunn Undergr Space Technol* 71: 115-125
<https://doi.org/10.1016/j.tust.2017.08.015>
- Valdenebro JV, Gimena FN (2018) Urban utility tunnels as a long-term solution for the sustainable revitalization of historic centres: the case study of Pamplona-Spain. *Tunn Undergr Space Technol* 81: 228-236.
<https://doi.org/10.1016/j.tust.2018.07.024>
- Wang X, Wang M, Zhang M, Ming H (2008) Theoretical and experimental study of external water pressure on tunnel lining in controlled drainage under high water level. *Tunn Undergr Space Technol* 23: 552-560.
<https://doi.org/10.1016/j.tust.2007.10.004>
- Yang C, Peng F (2016) Discussion on the development of underground utility tunnels in China. *Proc Eng* 165: 540-548.
<https://doi.org/10.1016/j.proeng.2016.11.698>
- Zhang N, Shen JS, Zhou AN, Arulrajah A (2018) Tunneling induced geohazards in mylonitic rock faults with rich groundwater: A case study in Guangzhou. *Tunn. Undergr. Space Technol* 74: 262-272.
<https://doi.org/10.1016/j.tust.2017.12.021>
- Zou YL, He C, Zhou Y, et al. (2013) Statistics and Cause Analysis of Leakage Diseases in Operating Expressway Tunnels. *J Highway Transp Res Dev* 30: 86-101. (In Chinese)
<https://doi.org/10.3969/j.issn.1002-0268.2013.01.016>